Available online at www.sciencedirect.com
SCIENCE DIRECT
Journal of Colloid and Interface Science 298 (2006) 825–831
JOURNAL OF Colloid and Interface Science
www.elsevier.com/locate/jcis

Surface characterizations of mono-, di-, and tri-aminosilane treated glass substrates

E. Metwalli [a,b,*], D. Haines [c], O. Becker [b], S. Conzone [c], C.G. Pantano [a]

[a] *Department of Material Science and Engineering, Material Research Institute, The Pennsylvania State University, 198 MRI Building, University Park, PA 16802, USA*
[b] *Schott AG, Hattenbergstr. 10, D-55014, Mainz, Germany*
[c] *Schott North America Inc., 400 York Avenue, Duryea, PA, USA*

Received 16 December 2005; accepted 17 March 2006
Available online 27 March 2006

Abstract

The surface properties and structure of mono-, di-, and tri-aminosilane treated glass surfaces were investigated using surface analytical techniques including X-ray photoelectron spectroscopy (XPS), Raman spectroscopy, atomic force microscopy (AFM), and streaming potential. An optimized dip-coating process was demonstrated to produce roughly silane monolayer coverage on the glass surface. The surface charge measurements indicated that aminosilanization converts the glass surface from negative to positive potentials at neutral pH values. Higher positive streaming potential was observed for tri- compared with mono- and di-aminosilane treated glass surfaces. For all aminosilane treated glass samples, the high-resolution N 1s XPS spectra indicated a preferential orientation of the protonated amino-groups towards the glass surface whereas the free amino groups were protruding outward. This study aimed to obtain uniform, reproducibly thin, strongly adhering, internally cross-linked, and high positively charged aminosilane-coated glass surfaces for the attachment of DNA fragments used in microarraying experiments.
© 2006 Elsevier Inc. All rights reserved.

Keywords: Glass surface; Aminosilane; Microarrays; XPS; Molecular orientation; Raman

1. Introduction

Thin films of functional organosilane molecules on solid surfaces have found important industrial applications, such as supports for biomolecules [1] and catalysts [2], advanced composite materials [3], and synthesis of chromatographic supports [4]. With the general formula $(X)_3SiY$, where X is an alkoxy ($–OCH_3$ or $–OCH_2CH_3$) or halogen (–Cl) ligand and Y is an organofunctional group (aminopropyl, methacryloxy, glycidoxy, vinyl, etc.), the bifunctional organosilane molecules undergo two different types of chemical reactions. The alkoxy groups (–OR) hydrolyze in an aqueous environment, producing hydroxyl groups, one or more of which may undergo condensation and elimination reactions with surface –OH groups commonly found on inorganic surfaces as well as on neighboring organosilane molecules. The reactivity of the Y-functional group is utilized for attachment of additional moieties or as a coupling agent to bond with secondary surfaces [5–7].

Generally, alkoxysilane molecules hydrolyze rapidly in water forming isolated monomers, cyclic oligomers, and large intramolecular cyclics [5,8,9]. The control over which species predominates is determined by silane type, concentration, pH, temperature, storage condition, and time. For instance, the low concentration (1%, w/w) of aminopropyltriethoxysilane (APS) in aqueous solution ($pK \approx 8.5$) is stable and forms trisilanol monomers and very low molecular weight oligomeric cyclics [5]. The adsorption mechanism of APS on glass surfaces has been extensively studied [10–14]. In addition to the siloxane (Si–O–Si) linkages [10], very strong hydrogen bonds between amino groups of the silanes and the surface silanol groups are formed [15]. The H-bonding has been proved using FTIR [11], ^{13}C MAS NMR [12], and X-ray photoelectron spectroscopies [13,14]. Furthermore, the amino group itself is believed to act

* Corresponding author. Current address: Physics Department, Technische Universität München, James-Franck-Str. 1, D-85747 Garching, Germany. Fax: +49 089 28912473.
E-mail address: ezz.metwalli@ph.tum.de (E. Metwalli).

0021-9797/$ – see front matter © 2006 Elsevier Inc. All rights reserved.
doi:10.1016/j.jcis.2006.03.045

as a catalyst and enhance the adsorption rate of APS molecules on the glass surface [16,17].

It has been experimentally observed [18] that APS-coating layer on solid surface is not uniform but instead forms "islands" with dimensions large enough to be detected by SEM. The polysiloxane structure inside such islands is also non-uniform and is composed of a 3D graded network (the cross-linking density is graded along the island thickness) [19,20]. Inside such islands, the inner part forms a layer of silane monomers that is highly cross-linked with both the substrates and top silane molecules. The outer part, which is exposed to environment, has open structure with low cross-linking density and high fraction of loosely bonded molecules [6]. From the technological point of view, silane coatings for adhesion promotion applications should offer a robust and internally cross-linked layer of reproducible thickness. Such characteristics cannot be achieved for multilayer coatings with high possibility of "islands" formation. For example, DNA microarrays utilizing organosilane coatings often have significant experimental variability due to the various difficulties in producing uniform coatings [21].

In the present study, mono-, di-, and tri-aminosilanes are applied to glass surface using an optimized dip-coating process with the objective to obtain a robust monolayer coating with high accessible number of amino groups and high positive surface charge for DNA microarray applications. We have generated a calibration curve for the thickness, thus the silane-coating layer on glass samples can be semi-quantitatively measured using X-ray photoelectron spectroscopy (XPS). The properties and structure of the silane-coating layers were characterized using XPS, atomic force microscopy (AFM), Raman spectroscopy, and streaming potentials. Furthermore, we have explored the molecular orientations of different aminosilane molecules on the glass surface using angle resolved XPS N 1s analysis.

2. Materials and methods

2.1. Materials

Low self-fluorescence microscopic slides ($1 \times 25 \times 75$ mm) were supplied by Schott AG (Jena, Germany). Glasses include borosilicate 1, borosilicate 2, soda-lime silicate, and synthetic fused silica. Silicon wafers were also used in this study (n-type; Wafernet, San Jose, CA) whereby the surface was comprised of a thin (40 ± 0.5 Å) SiO_2 layer. Three aminosilane compounds (Gelest Inc.) were used without further purification: 3-aminopropyltriethoxysilane (APS), N-(2-aminoethyl)-3-aminopropyltrimethoxysilane (EDA), and (3-trimethoxysilylpropyl) diethylenetriamine (DETA). The chemical structures of these compounds are schematically represented in Fig. 1. Concentrated HCl and NaOH solutions (research grade; Aldrich Chem. Co.) were diluted to obtain the desired concentrations. The solvents were HPLC grade (Aldrich Chem. Co.) and used without further purification. All references to H_2O in the text refer to water obtained from a Nanopure^{TM} purification system (resistivity >18 MΩ cm).

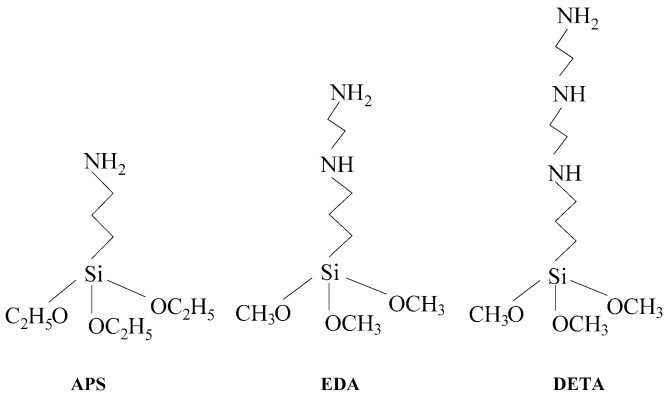

Fig. 1. Schematic structures for 3-aminopropyltriethoxysilane (APS), N-(2-aminoethyl)-3-aminopropyltrimethoxysilane (EDA), and (3-trimethoxysilylpropyl) diethylenetriamine (DETA).

2.2. Sample preparation

2.2.1. Dip coating

Glass substrates were cleaned using a general glass cleaning protocol: immersion in NaOH (2.5 M) solution for 24 h, sonication in H_2O for 10 min, immersion in HCl (0.1 M) for 15 min, sonication in H_2O for 10 min and immersion in methanol for 5 min prior to the silanization step.

Silanization of the samples were performed by dip coating in 1% aqueous solutions of silane for 15 min. Post-treatment steps include shaking in methanol for 5 min, rinsing in H_2O for 10 min and finally spin drying (2000 rpm) for 5 min. The coated slides were baked at 110 °C for 15 min and stored in a vacuum desiccator prior to analysis.

2.2.2. Pulsed CVD coating

Due to the small differences between the refractive index of both glass substrate and the organosilane film, ellipsometry cannot measure the organosilane film thicknesses on glass surfaces [22]. To obtain information on the thickness of the silane film, a silicon wafer was substituted for the glass substrates. Using a pulsed CVD technique (ThinSonic pulsed ultrasonic CVD; Sono-Tech Corp.), different APS film thicknesses were deposited on silicon wafers. The pulsed ultrasonic method is a process in which the precursor is delivered to the ultrasonic nozzle through a series of automatically controlled solenoid valves. The experimental apparatus is described in detail elsewhere [23]. The precursor is atomized at the tip of the nozzle and introduced into a low-pressure reaction chamber in a near-vapor-phase state (∼15 μm drop diameter). Nozzle power, volume of pulses and number of pulses were varied to obtain the desired coating thicknesses. All of the silicon wafer substrates were first cleaned in NH_4OH:H_2O_2:H_2O (1:1:5) solution before the silane deposition step. The substrates were heated (120 °C) in situ for 15 min prior to the pulses injections. A control sample was prepared as described above excluding the deposition step. Silane layer thicknesses on the Si wafer samples were measured using an ellipsometer (Gaertner L116C). Dip-coated Si wafer samples were also prepared by immersion in 1% APS (aqueous) solution for 15 min; some samples were dried under N_2 without any post-washing steps,

other samples were rinsed in methanol and H_2O for 5 min prior to a N_2 blow drying step.

2.3. Analysis

2.3.1. X-ray photoelectron spectroscopy

X-ray photoelectron spectroscopy (XPS) was performed on the silane-coated samples using a Kratos analytical XSAM 800pci instrument. Photoelectrons were excited using Mg$K\alpha$ 1253.6 eV X-ray irradiation. Spectra were collected at an electron emission angle of 80° with respect to the sample surface plane. High-resolution scans (40 eV pass energy) of all surface elements were taken and reported as an average of two samples for each condition. The sampling depths at 80° electron take-off angles were estimated to be 5–10 nm [24].

Nitrogen 1s high-resolution XPS scans of different samples were collected from XPS Kratos Analytical Axis Ultra (a monochromatic AlK_a X-ray source operated at 450 W). Charge neutralization was provided by the Kratos charge neutralization system, which has the unique ability to provide consistent charge compensation even at near grazing take-off angles. All neutralizer parameters remained constant during analysis. Nitrogen 1s high-resolution spectra of APS-, EDA-, and DETA-coated glass samples were collected at a low pass energy of 5 eV. The C 1s peak (285 eV) was used as a binding energy reference. For each photoelectron take off angle from 20° to 90°, a fresh sample was used to avoid the X-ray source damage of the sample surface.

2.3.2. Streaming potential

The surface charge on the glass surfaces was measured using streaming potential analysis. Adapting the procedure described by Walker et al. [25] the protocol for the streaming potential measurements was as follows: the cell was first cleaned with RO water, then DI water, ethanol, and then DI water again before loading the flat glass sample. The glass-substrate containing cell was flushed with DI water (7 L), then with 1 L of electrolyte solution (0.01 M KCl). Once thoroughly flushed, the electrolyte solution (0.01 M KCl, 7 L, pH ∼ 7) was circulated through the cell for 20 min. Using HCl, the pH was first adjusted to the acidic level (pH 3) then followed by adjustment with KOH (0.1 and 0.01 M KOH) to higher pH levels. For each pH, the solution was circulated for 20 min. The streaming potential was measured using an electrometer (Keithley 6517) as an average of the readings during the flow of 1 L solution.

2.3.3. Raman spectroscopy

Raman spectrum was collected with a double stage Dilor XY spectrometer equipped with a Princeton Instruments Model LN/CCD-1024 detector. A Spectra-Physics model 164 argon ion laser was used for excitation at 514 nm. The laser was focused at an angle of 35° onto the sample with a spot size of approximately 10 μm. The Raman spectrum was collected for 300 s at a laser power of 25 mW. Data acquisition was conducted under computer control.

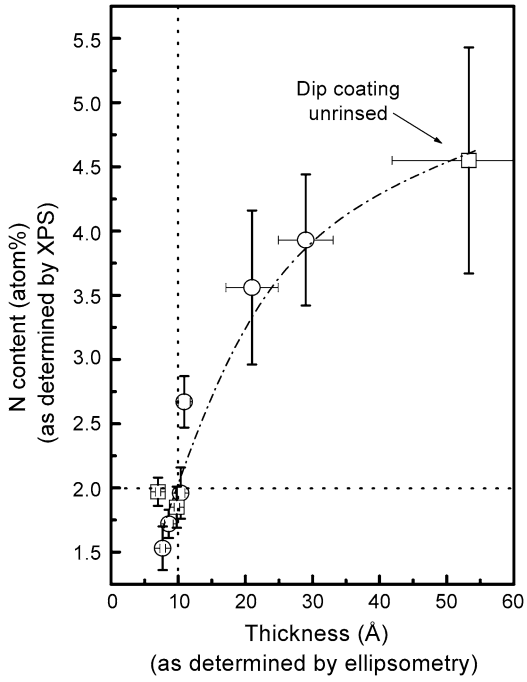

Fig. 2. The thicknesses of silane layer (by ellipsometry) on Si wafer substrate (covered with 40 ± 0.5 Å SiO_2 layer) versus the surface N content (by XPS). (○) Pulsed CVD-coated, (□) dip-coated samples.

2.3.4. Atomic force microscopy

AFM measurements were collected for aminosilane-coated glass samples using a Digital Instrument Dimension™ 3100 Scanning probe microscope. Five spots (5 μm × 5 μm) were scanned to ensure representative areas. All scans were done in the Tapping Mode™.

3. Results

3.1. Monolayer surface coverage

The surface N content of the APS-coating layer as determined using XPS technique versus the silane layer thickness as determined using ellipsometry for various APS-coated silicon wafer samples is shown in Fig. 2. The nitrogen content of 1.5–2 (±0.2) atom% is corresponding to roughly a monolayer silane coverage of 7–10 Å (contrasted to the length of fully stretched APS molecule which is 9 ± 1 Å [26]). As the APS layer thickness increases, the surface N content correspondingly increases (Fig. 2), then tends to level off as it approaches saturation within the analysis depth of the XPS measurements. It is also worth noting that as the APS layer thickness increases beyond a monolayer, the standard deviation of the thickness (error bars in Fig. 2) significantly increases due to the non-uniform multilayer organosilane deposition (island formation).

For APS dip-coated silicon wafer samples (indicated by the square labels in Fig. 2), it is obvious that the post-treatment steps (rinsing in methanol followed by 5 min rinsing in H_2O) was effective enough to remove all weakly bounded physisorbed molecules and to obtain a smooth, and reproducible coated surface; this is revealed by the small error bars of the rinsed samples compared to the unrinsed data point in Fig. 2.

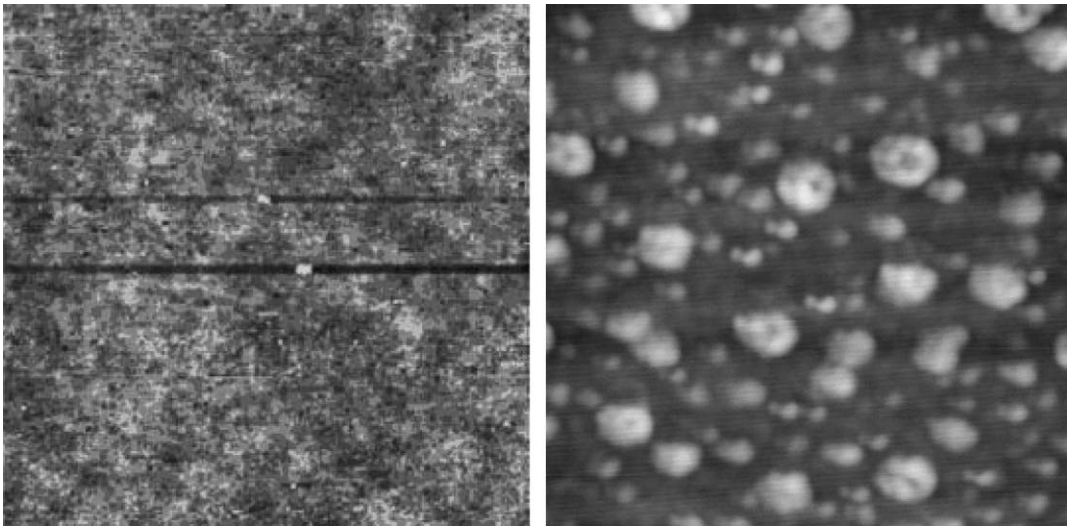

Fig. 3. AFM images ($5 \times 5\ \mu m^2$) of rinsed (left) and unrinsed (right) APS dip-coated glass surface.

Table 1
Surface compositions (atom%) of APS treated glasses

Element	Silica glass		Soda-lime glass		Borofloat 1 glass		Borofloat 2 glass	
	Clean	APS	Clean	APS	Clean	APS	Clean	APS
O	65.94	57.12	66.7	61.34	65.53	57.83	62.64	53.7
C	3.25	12.48	3.91	9.24	1.99	9.66	3.47	12.45
Si	30.8	29.08	26.79	25.7	27.55	25.91	19.06	18.51
B	–	–	–	–	3.45	3.45	8.32	7.75
Na	–	–	1.21	0.82	0.37	0.49	–	–
Al	–	–	0.62	0.69	1.02	0.82	5.06	4.57
Sn	–	–	–	–	0.1	0.08	–	–
Ca	–	–	0.7	0.64	–	–	–	–
Ba	–	–	–	–	–	–	1.45	1.05
N	–	1.33	–	1.57	–	1.75	–	1.97

AFM images (Fig. 3) demonstrate the silane "islands" formation for the unrinsed versus the rinsed APS-coated samples.

Table 1 shows the surface compositions of various APS dip-coated glass samples. Independent of various surface glass chemistries (silica, soda-lime, borosilicate 1, and borosilicate 2), APS silanization process that followed by post-washing steps results in roughly a monolayer APS layer on the glass surface as revealed by the surface N content of 1.33–2 atom%. Furthermore, the root mean square roughness (rms) values of <0.15 nm indicates relatively smooth surfaces for all APS-coated glass samples. The rms values of APS multilayers coated (unrinsed) samples were >0.8 nm.

The tri-amino (DETA) coated glass (borofloat 1) samples have almost 3 times as much surface N content (4.5–5.5 atom%) as the corresponding APS-coated (1.3–2 atom%) sample. In addition, the AFM data reveals a slightly smoother APS-coated sample (rms = 0.15 nm) compared with DETA-coated one (rms = 0.207 nm). The differences in roughness between DETA and APS treated samples may be attributed to differences in the silane linker length (DETA molecule is almost 3 times longer than APS molecule). From the above results, it is inferred that our silanization protocol most likely produces monolayer coverage for amino-coated glass samples.

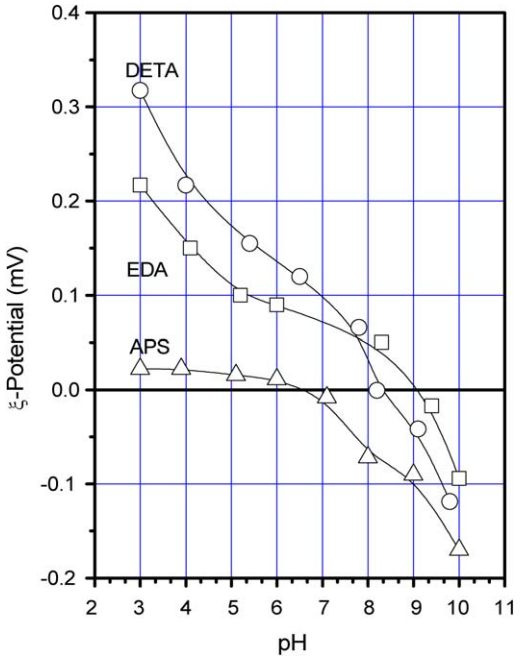

Fig. 4. Streaming potentials of aminosilane treated glass surface. The lines are drawn as guides for the eye.

3.2. Surface charge

Mono- (APS), di- (EDA), and tri- (DETA) aminosilanes were deposited on flat glass surface (glass slides). The effect of the three silanes on the average surface charge was determined using streaming potentials. Fig. 4 demonstrates that the treating of glass surfaces with aminosilanes creates a positive surface charge at pH $\geqslant 7$. For amino-coated surface samples, DETA creates a higher positive potential than APS treated samples. But clearly, surface potential is a distinguishing characteristic of DETA (versus APS) on flat surfaces at any pH.

Raman spectrum collected for DETA silane treated flat glass (borofloat 1) surface (Fig. 5), indicates the presence of posi-

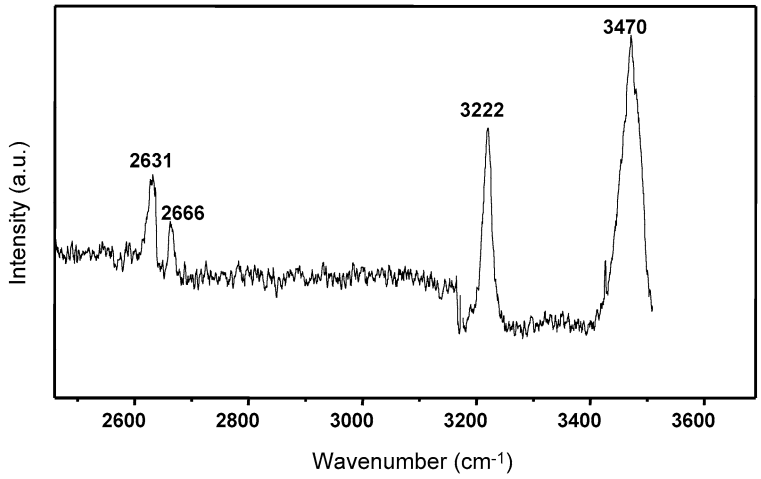

Fig. 5. Raman spectra from DETA-coated glass sample.

tively surface charged moieties. Strong peaks at 2631, 2666, and 3222 cm^{-1} are assigned [27] to $=NH^{+}–$, $–NH_2^{+}–$, and $–NH_3^{+}$ groups respectively confirming the presence of various protonated amino groups. Also, there is a high number of free N content on the DETA treated glass surface as revealed from high-intensity peak at 3470 cm^{-1}. Raman spectrum of APS-coated silica surface is described in detail elsewhere [28]. For APS treated surface, the absence of the characteristic free NH_2 modes (3470 cm^{-1}) is attributed [28] to the H-bonding between almost all the NH_2 groups and the nearby attached hydrogen atoms. The absence of the C–H vibrational modes (2800–3000 cm^{-1}) in the DETA treated glass sample may be attributed to the linkage of the lone pairs of electron on the free amino groups to the H atoms on the CH_2 units. Generally, both surface charge measurements and Raman spectrum confirm the positive surface charge characteristic of aminosilane treated glass samples.

3.3. Silane molecular orientations

Fig. 6 shows the nitrogen 1s high-resolution spectra of APS-, EDA-, and DETA-coated glass samples. Both of protonated (401.5 eV) and non-protonated (399 eV) amine groups are clearly evident in the XPS spectra (Fig. 6). The formation of protonated amine is due to the reaction of the silane $NH_2–$ (or –NH–) groups with the OH groups on the glass surface and/or with OH groups on other silane molecules in an acid–base reaction (the specific interactions cannot be uniquely determined with XPS). Fig. 6 shows that the protonated amine peaks (∼401 eV) are more intense in the order APS > EDA > DETA, but the higher number of N-groups and larger molecular size for both DETA and EDA compared with APS molecule must be considered to draw any structural inference. For different silanes (APS, EDA, and DETA), as the take off angle decreases from 90 to 20 (the analysis depth is smaller), the N^{+}/N ratio decreases. This indicates a preference for the protonated amine to be oriented towards the glass surface, and the non-protonated amine to be oriented away from the surface. These results are inconsistent with the XPS results on APS treated fibers reported by Fowkes et al. [13] and indicate the interactions between amino groups of APS silane molecules and the OH moieties at the surface interface.

4. Discussion

The creation of a uniform silane monolayer allows, in theory, the functional moiety (Y) of the silane to crosslink with subsequently deposited biomolecules in a reproducible manner. Successful and reproducible deposition of a uniform silane monolayer on glass substrates depends not only on the silanization conditions (temperature, concentration, solvents, hydration and reaction time), but also on both pre- and post-treatment processes.

The pre-treatment cleaning of the glass before silane deposition has three important objectives: elimination of contamination, control of the surface composition, and hydroxylation. Many studies [29–31] of glass cleaning have been reported, but there is no universal cleaning protocol. In principle, the clean hydroxylated glass surface should be energetically “homogeneous” in order to obtain a uniform surface coating.

Following the silanization step, the post-treatment (washing) step is also important to remove the weakly physisorbed silane molecules. Hozumi et al. [32] have used strong base (NaOH) and acid (HNO_3) as post-washing solutions, however, our study and earlier studies [26,33] indicate that the loosely bounded silane molecules are easy to remove with alcohols and/or H_2O washings immediately after the silanization step. Structural differences between chemisorbed and physisorbed silane molecules have been investigated using FTIR [34]. Chemisorbed molecules are attached to the surface through Si–O–Si linkages and hydrogen bonds (between the amino and the surface OH groups). Physisorbed molecules are only intermolecularly bonded via Si–O–Si to each other with free NH_2 groups. Such structural characteristics of the physisorbed molecules indicate that these molecules are weakly bonded and easy to remove by simple washing procedure. Heat treatment is the final step in the silanization process that helps to inter-crosslink the silane molecules on the surface through the elimination of H_2O molecules forming a relatively more robust silane layer.

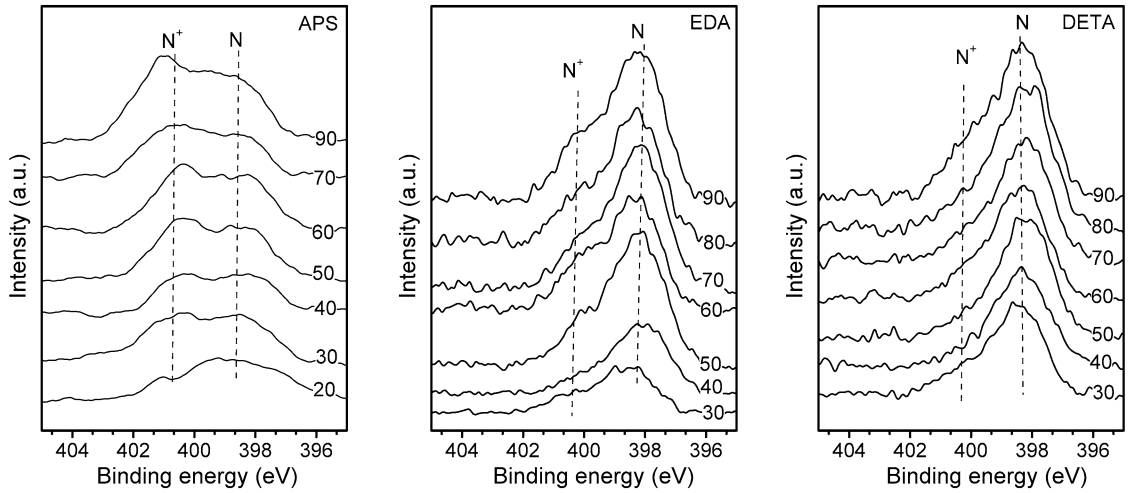

Fig. 6. N 1s high-resolution XPS spectra of APS-, EDA-, and DETA-coated D263 glass samples. Experiments were performed at different photoelectron take-off angles. Analysis depth increases as the angel increases. Only XPS spectra of APS-coated samples are smoothed (averaging the noisy) due to small dwell time used. Other XPS spectra collected throughout this study have not been smoothed since they are all performed at the same conditions (high dwell time).

For DNA microarray applications, the role of the amino-functional groups of the silane-coating layer in the attachment process of biomolecules (DNA or nucleotides) to glass surface is known [35–37] to be crucial, however, it is not known whether the best coating performance can be achieved with just a monolayer of aminosilane or whether multilayers are necessary. Wieringa [38] applied APS to glass surfaces and compared between the DNA microarray assay performances of three different silane layer thicknesses (monolayer, 2–3 layers, and multilayers) deposited using different techniques. According to his study, chances of incomplete coverage of the monolayer coating, and poor reproducibility for multilayers coverage, make 2–3 layers thick film the best coating for bimolecular attachment. However, DNA array technology possesses many sources of technical variability that are an obstacle to obtaining high quality data set [39]. To minimize such data inconsistency, the need for extremely uniform silane layer (that should have fairly equal binding ability throughout the glass surface) is essential. Such uniformity can only be achieved through one-molecule thick layer coverage of the silane on the glass surface. Thicker films can have three-dimensional aggregate structures or "islands" of multilayers and hence results in a large variability in the performance of the DNA assays [21].

The calibration curve for silane layer thickness versus the surface N content generated in our study, indicates that 1.5–2 atom% N corresponds to a monolayer (7–10 Å) of APS silane (Fig. 2). This is in agreement with a previous study [40] where a monolayer (11 Å) APS on glass surface is deposited by dip coating in aqueous APS solution with surface loading of 6.4 silanes/nm^2. The dip-coating protocol used in our study roughly generates an APS monolayer coverage on the glass surface (Table 1) as revealed by both N content (1.3–2 atom%; probed using XPS) and the smooth surfaces (rms < 0.15 nm; probed using AFM). The monolayer coverage was also assumed for multi-aminosilanes (EDA and DETA) as revealed from the smooth surfaces (rms < 0.21 nm) with no indication of silane "islands" formation.

Surface charge of the solid support is also an important characteristic for DNA microarray application. The electrostatic attractions between the negatively charged biomolecules (DNA or nucleotides molecules) and the positively charged surfaces help to fix the biomolecules on the surface prior to the immobilization step. The immobilization step is usually initiated by UV or heat cross-linking process to form strong covalent bonds between the biomolecules and the glass surface [41]. The streaming potential (Fig. 4) of the aminosilane treated glass surfaces changes from negative to positive values as the pH decreases. At pH $\geqslant 7$, the streaming potential values increase in the order DETA > EDA > APS. The positive charge characteristics of the aminosilane glass surface are attributed to the presence of protonated amino groups detected using both high-resolution N 1s XPS (Fig. 6) and Raman spectrum (Fig. 5). The high positive charge tendency of DETA compared with EDA and APS treated surfaces may be attributed to high surface N density of the multi-aminosilane treated surface with potentiality of large numbers of positive protonated amino groups. These streaming potential results cannot be further supported by the N^+/N ratios calculated from XPS spectra for various studied aminosilane treated glass surfaces (Fig. 6). The N^+/N ratio shows higher values for APS compared to DETA treated surfaces at all take off angles. The reason for such incompatibility between the XPS and streaming potential data may be attributed to some experimental procedure related issues. The surface charge (streaming potential) has been measured during exposure to aqueous environments, whereas the XPS data probe the "dry" surface. In addition, the differences in the molecular sizes and the number of amino groups make it difficult to compare between N^+/N ratios (by XPS) of the various aminosilanes treated surfaces especially when the protonated amino groups are mainly oriented towards the glass surface and away from the XPS detector.

Fig. 6 shows that the free amino groups (which are important for immobilization process of DNA molecules) have higher absolute intensities in the order DETA > EDA > APS. For mono-, di-, tri-aminosilane treated glass surfaces, as the XPS

take off angle decreases relative to the sample surface, the free-NH_2 group intensity increases which indicates a preferential orientation of the free amino groups away from the glass surface that would in theory, increases the binding susceptibility of the attached biomolecules to the coated glass surface.

5. Summary

The properties and structure of mono-, di-, and tri-aminosilane treated surfaces were investigated using multi-techniques surface characterization including XPS, Raman, AFM, and streaming potential. Stringent washing (using organic solvents followed by distilled water) immediately after the silanization step was effective to remove physisorbed molecules and produce a monolayer coverage of silane on the glass surface as revealed from N content and surface roughness data. The positive charge characteristics of the aminosilane modified surfaces are attributed to the formation of protonated amino groups via hydrogen bonding between amino groups and acidic OH groups on the glass surface as revealed from the peak at 401.5 eV in the high-resolution N 1s XPS spectra. Molecular orientations study indicates a preferential for protonated amino groups towards the glass surface while the free amino groups are protruding to the air-side. High positive streaming potential and large number of free amino-groups of the multi-aminosilane (DETA) compared to APS treated glass substrates indicate that the DETA treated glass surface offers advantageous surface properties for DNA microarray applications.

Acknowledgments

The authors thank Jeffrey R. Shallenberger and Vince Bojan for their technical assistance and fruitful discussion.

References

[1] L.A. Chrisey, G.U. Lee, C.E. O'Ferrall, Nucleic Acids Res. 24 (1996) 3031.
[2] A.J. Aznar, E. Ruiz-Hitzky, Colloid Polym. Sci. 270 (1992) 165.
[3] B. Arkles, J. Steinmetz, J. Hogan, Mod. Plast. Int. 49 (1987) 126.
[4] D. Mislovicova, I. Novak, M. Pasteka, J. Chromatogr. 543 (1991) 9.
[5] E.P. Plueddenmann, Silane Coupling Agents, Plenum, New York, 1991.
[6] D. Olmos, J. Gonzalez-Benito, A.J. Aznar, J. Baselga, J. Mater. Process. Technol. 143–144 (2003) 82.
[7] K.L. Mittal, Silanes and Other Coupling Agents, vol. 2, VSP, Utrecht, 2000.
[8] H. Ishida, Polym. Compos. 5 (1984) 101.
[9] H. Ishida, J.L. Koenig, Polym. Eng. Sci. 18 (1978) 128.
[10] H.-J. Kang, F.D. Blum, J. Phys. Chem. 95 (1991) 9391.
[11] M. Child, M. Heywood, S. Pulton, G. Vicary, G.H. Young, J. Colloid Interface Sci. 89 (1982) 203.
[12] K.M.R. Kallury, P.M. Macdonald, M. Thompson, Langmuir 10 (1994) 492.
[13] F.M. Fowkes, D. Dwight, D. Cole, J. Non-Cryst. Solids 120 (1990) 47.
[14] J.R. Schallenberger, E. Metwalli, C.G. Pantano, F.N. Tuller, D.F. Fry, Surf. Interface Anal. 35 (2003) 667.
[15] P. Arora, J. Matisons, A. Provatas, R. Smart, Langmuir 11 (1995) 2009.
[16] J.J.P. Blitz, R.S. Shreedhara Murthy, D.E. Leyden, J. Colloid Interface Sci. 126 (1988) 387.
[17] P. Trens, R. Denoyl, J. Rouquerol, Langmuir 11 (1995) 551.
[18] E.T. Vandenberg, L. Bertilsson, B. Liedberg, K. Uvdal, R. Erlandsson, H. Elwing, I. Lundström, J. Colloid Interface Sci. 147 (1991) 103.
[19] D. Wang, F.R. Jones, P. Denison, J. Mater. Sci. 27 (1992) 36.
[20] D. Wang, F.R. Jones, J. Mater. Sci. 28 (1993) 2481.
[21] R.J. Redkar, S.D. Conzone, L.A. Burzio, D.H. Haines, in: D. Thangadurai, W. Tang (Eds.), Genes, Genomes and Genomics, Regency Publications, New Delhi, 2005.
[22] C. Bungay, VUV-VASE Measurements of Thin Organic Films, J.A. Woollam Co., Personal communication, 2003.
[23] D. Krumdieck, R. Raj, Surf. Coat. Technol. 141 (2001) 7.
[24] D. Briggs, M.P. Seah, Practical Surface Analysis by Auger and X-Ray Photoelectron Spectroscopy, Wiley, New York, 1983, p. 363.
[25] S.L. Walker, S. Bhattacharjee, E.M.V. Hoek, M. Elimelech, Langmuir 18 (2002) 2193.
[26] D.F. Siqueira Petri, G. Wenz, P. Schunk, T. Schimmel, Langmuir 15 (1999) 4520.
[27] G. Socrates, Infrared and Raman Characteristic Group Frequencies, third ed., John Wiley & Sons Inc., New York, 2001, p. 108.
[28] C.A. Davis, P.R. Graves, P.C. Healy, S. Myhra, Appl. Surf. Sci. 72 (1993) 419.
[29] J.J. Cras, C.A. Rowe-Taitt, D.A. Nivens, F.S. Ligler, Biosens. Bioelectron. 14 (1999) 683.
[30] K. Shirai, Y. Yoshida, Y. Nakayama, M. Fujitani, H. Shintani, K. Wakasa, M. Okazaki, J. Snauwaert, B. Van Meerbeek, J. Biomed. Mater. Res. (Appl. Biomater.) 53 (2000) 204.
[31] E.C. Onyiriuka, C.B. Moore, F.P. Fehlner, N.J. Binkowski, D. Salamida, T.-J. King, J.G. Couillard, Surf. Interface Anal. 26 (1998) 270.
[32] A. Hozumi, Y. Yokogawa, T. Kameyama, H. Sugimura, K. Hayashi, H. Shirayama, O. Takai, J. Vac. Sci. Technol. 19 (2001) 1812.
[33] S.R. Wasserman, Yu.T. Tao, G.M. Whitesides, Langmuir 5 (1989) 1074.
[34] S.R. Culler, H. Ishida, J.L. Koenig, J. Colloid Interface Sci. 106 (1985) 334.
[35] J.D. Hoheisel, M. Vingron, Res. Microbiol. 151 (2000) 113.
[36] J.G. Hacia, Nat. Genet. 21 (1999) 42.
[37] D. Gerhold, T. Rushmore, C.T. Caskey, Trends Biochem. Sci. 24 (1999) 168.
[38] R.M. Wieringa, Ph.D. thesis, Univ. of Gromigen, The Netherlands, 2000.
[39] M.J. Hessner, L. Meyer, J. Tackes, S. Muheisen, X.J. Wang, BMC Genomics 5 (2004), Art No. 53.
[40] D.G. Kurth, T. Bein, Langmuir 9 (1993) 2965.
[41] S. Conzone, C.G. Pantano, Mater. Today 7 (2004) 20.